

Modeling IR absorption spectra of the carbon dioxide within the ν_2 absorption band

V.F. Golovko

*Institute of Atmospheric Optics,
Siberian Branch of the Russian Academy of Sciences, Tomsk*

Received June 29, 2005

In this study I have used an original technique to allow for the super-Lorentzian absorption within central portions of the Q-branch profiles and in the far wings of the absorption lines in describing IR absorption spectra of the carbon dioxide within wide frequency region of ν_2 absorption band from 550 to 1200 cm^{-1} . The calculated results are compared with the values of the absorption coefficient measured under conditions of broadening by nitrogen at pressures from 70 to 200 atm and temperatures from 200 to 300 K. A simple algorithm of relevant calculations has been tested and it was shown that it can successfully be used in modeling transmission functions of the Earth's atmosphere and atmospheres of other planets.

Introduction

Recently an increased interest has been shown in modeling transmission functions of the Earth's atmosphere that caused an essential progress achieved in such studies under various programs on radiation research (see, for instance, Refs. 1 and 2). All these studies point out special importance of the account of contribution of non-Lorentzian absorption to formation of the absorption line shape due to continuum absorption, mixing of lines and branches within the resonance portion of the line contour. The problem on the role of under-Lorentzian absorption in the formation of the absorption line wings has also become important. The last two problems have recently been treated in Refs. 3 to 5 by Niro and co-workers. They have combined the experimental and theoretical studies³ with the following tests in modeling the atmospheric absorption spectra.^{4,5} The basis for such combined research has been laid in their earlier studies.⁶⁻⁹ In addition to the above-mentioned studies there are many other laboratory studies demonstrating the importance of the account of such a behavior of the line shape in the entire infrared spectrum.

In this study we have applied the technique we proposed earlier for calculating contributions of far line wings¹⁰ and super-Lorentzian absorption in the centers of the absorption line contours^{11,12} to modeling absorption within the ν_2 band by use, as examples, those studied experimentally and modeled in Ref. 3. Like in Refs. 11 and 12, simple methods of calculations are being developed in this study with the peculiar feature that here we study the broadening of carbon dioxide spectra by nitrogen, instead of the broadening in the CO_2 -He mixture.

1. General scheme of calculations

The calculations are based on line-by-line calculation technique with the use of non-Lorentzian

contour of an individual i th line $\Phi_i(\omega, p, T)$ as a function of frequency ω . Under the external conditions characterized by the pressure p and temperature T the contour is presented in the form of a product of the Lorentzian line shape $L_i(\omega, p, T)$ and some factor-function $\Xi_i(\omega, p, T)$ (see Refs. 11 and 12):

$$\Phi_i(\omega, p, T) = L_i(\omega, p, T)\Xi_i(\omega, p, T). \quad (1)$$

The factor-function Ξ_i , in its turn is presented as a product of two functions:

$$\Xi_i(\omega, p, T) = \Gamma_i(\omega, p, T)K_i(\delta\omega_i, T). \quad (2)$$

The factor K describes the far wings. It depends on the frequency shift $\delta\omega_i = \omega - \omega_i$ from center frequency of the line contour ω_i and includes the exponential, according to hypothesis from Ref. 10, temperature dependence. For the cases of right-hand ($\delta\omega \geq 0$) and left-hand ($\delta\omega < 0$) parts of the contour it correspondingly has the following views¹⁰:

$$K_i(\delta\omega_i, T) = n_r = 1/(\exp(Nhc\delta\omega_i/kT) + 1), \quad (3)$$

$$K_i(\delta\omega_i, T) = n_l = 1 - n_r. \quad (4)$$

The function Γ_i is introduced to describe the narrowing of the line contours at high enough pressures p , exceeding critical values $p_s^{(i)}$ characteristic of each i th line. Its analytical view is unknown and following our earlier work¹⁰ it can be presented in the pointwise form as follows

$$\Gamma_{i,k}(\omega) = \left(\frac{1}{4}\right)^{x_{i,k}}. \quad (5)$$

If we omit the subscript i in expression (5) and divide the entire frequency interval of a line wing, from zero to infinity in the units of some line half-width ξ^a , into $n + 1$ segments

$$\delta\omega^{(k)} = z_k \xi^a,$$

where $k = 0, 1, \dots, n$, then the exponent x_k in expression (5) can vary over a continuous series of interpolated values within each k ($k > 0$) interval. The function (5) can be set by an array of discrete $n + 1$ values and the limits of the exponent intervals can be defined as

$$y_k = \log_{0.25} \left(\Gamma(\delta\omega^{(k)}) \right).$$

Then the continuous sequence of the exponent values within each of the intervals can be found by the interpolation formula for each $0 < k < n + 1$:

$$x_k(\omega) = y_k + \frac{z_k \xi^a - |\omega - \omega_i|}{(z_k - z_{k-1}) \xi^a} (y_{k-1} - y_k), \quad (6)$$

provided that $z_{k-1} \xi^a \leq |\omega - \omega_i| < z_k \xi^a$. In the case of an extremely far wing, when $k = n + 1$, we have $x_k = y_n = y_{n+1}$, where y_{n+1} is the exponent value for the case of infinitely long wing.

The superscript of the value ξ^a means an asymptotic behavior of some line half-width ξ , which we shall introduce later. Its dependence on pressure

$$\xi^a(p) = \xi_0^a + r \gamma^L(1 \text{ atm}) p \quad (7)$$

is less steep than in the case of usual Lorentzian half-width

$$\gamma(p) = \gamma(p = 1 \text{ atm}) p,$$

that means that the value r in expression (7) is less than unity. Since the values of ξ_0^a are above zero the straight lines $\xi^a(p)$ and $\gamma(p)$ should cross at some point p_s and all the pressure values $p < p_s$ can be called moderate. By introducing the ratio between the Lorentzian and asymptotic half-widths

$$r_i(p) = \gamma^L(p) / \xi_i^a(p),$$

one can take, at moderate pressure values, the boundary exponents for an individual i th line in the following form

$$y_{i,k}(p) = \log_{0.25} \{ 2 + (\Gamma_i(\delta\omega_k) - 2) r_i(p) \} \quad (8)$$

for all values $\Gamma_i(\delta\omega_k) > 2$, which, of course, belong to the central part of the line contour. For $\Gamma_i(\delta\omega_k) < 2$, that is in the line wing, the factor-function (8), in our algorithm, is the same as at high pressures.

Figure 1 presents different contours of an isolated line for the Q30 line from the ν_2 band, as an example. Our calculated data we compare with the Lorentzian contours and half-widths both usual $\gamma_{Q30}^L(p)$ and the asymptotic $\gamma_{Q30}^a(p)$. We use the following 6 pairs of values $k(n = 5)$ for the values $\{\Gamma\}_{k=0}^n = 3.7; 3.2; 2.6; 2.0; 1.0; 0.1$ from expression (5) at each value of the frequency

$|\omega - \omega_0|_k = z_k \gamma^a$, where $\{z_k\}_{k=0}^n = 0.00; 0.25; 0.58; 1.5; 4.00; 8.00$, respectively.

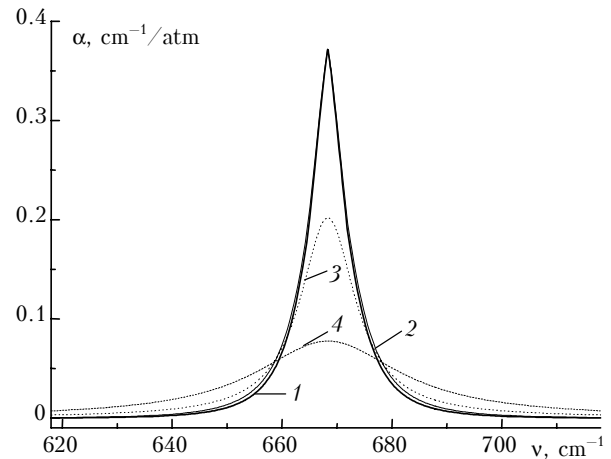


Fig. 1. An example of the line shape for Q30 line from the ν_2 band plotted with the account of the exponential factors (3) and (4) as well as without the account of this factor. Calculations have been made of the reduced absorption coefficient α for $p = 200$ atm and $T = 296$ K: curve 1 presents data calculated with the account of all factors; curve 2 shows data calculated without the account of the exponential factor; curve 3 demonstrates the data calculated using the Lorentzian and new half-width; curve 4 shows the data calculated using Lorentzian.

It is seen from Fig. 1 that at a pressure of 200 atm such a contour essentially differs from the Lorentzian curve. At that high pressure the influence of the exponential factor (3) and (4) on the line shape is quite noticeable. The absorption within the branches of the band is calculated using line-by-line method as a sum of contributions coming from individual lines under certain ambient conditions, the influence of which is considered below.

In contrast to usual Lorentzian half-width, which is directly proportional to pressure, at its moderate values, the half-width $\gamma(p)$ that enters the Lorentzian contour L from expression (1) approaches, as we suppose, to its asymptotic value $\gamma^a(p)$ at high pressures $p > p_s$. Here we calculate it by the following formula

$$\gamma(p) = \xi^a(p) \left[(2k(p) + 1) / (2(k(p) + 1)) \right], \quad (9)$$

where $k_i(p) = \gamma_i^L(p) / \xi_i^a(p_s)$ is the relative value of the Lorentzian half-width. The value p_s corresponds to the point of intersection between the straight line $\gamma_i^L(p)$ and the asymptotic curve $\xi_i^a(p)$, so that $k_i(p_s) = 1$. Under conditions of reduced pressures $p < p_s$ this value tends to a different asymptotic value, which in this scheme is usual Lorentzian half-width $\gamma^L(p)$ according, for example, to the formula

$$\gamma(p) = \gamma^L(p) \left[(k(p) + 2) / (2(k(p) + 1)) \right]. \quad (10)$$

Thus, having known the values of the half-width $\gamma(p)$ under conditions of moderate and high pressures one can describe the shape of an individual absorption line (1) at any pressure and then to calculate the absorption within a branch or a band at this pressure by use of line-by-line calculation method. We used this simple scheme in describing the absorption by the carbon dioxide in a mixture with helium.^{11,12} Below we shall make use of this scheme in similar calculations for CO₂ mixtures with nitrogen.

In our studies we have revealed that single asymptotic straight line is insufficient for describing the pressure dependence of the Lorentzian half-width in a wide range of pressures. To give a more precise description of this dependence, one can make use, for example, two asymptotic straight lines (7), $\xi^{a,I}$ and $\xi^{a,II}$ (see Fig. 2) and thus to obtain already an asymptotic curve ξ^a , which will define the asymptotic behavior of the half-width γ at high pressures.

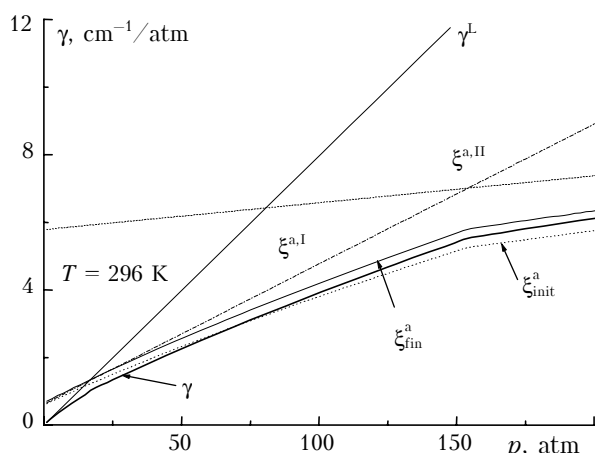


Fig. 2. Dependence of the half-width γ of an isolated Q30 line on pressure.

At high pressures $p \gg p_s$, its value (9) approaches the values defined by the curve $\gamma^L(p)$, while at low pressures it approaches following expression (10) the asymptotic values of the usual Lorentzian half-width $\gamma^L(p)$. The asymptotic curve is constructed using two asymptotic straight lines $\xi^{a,I}$ and $\xi^{a,II}$ with two sets of the parameters ξ_0^a and r . The resultant curve ξ_{fin}^a has been obtained from the initial one ξ_{init}^a by use of expression (14) given below.

2. Calculations of the central part of a line shape

Like in our papers 11 and 12 for the mixture of carbon dioxide and helium, the parameter ξ_0^a of the asymptotic behavior of the half-width (7) is calculated by the following formula

$$\xi_0^a = \xi_i^a(0) = A\Delta\omega_i, \quad (11)$$

where A is a constant; $\Delta\omega_i$ is the mean spectral distance between the i th and two neighbor lines of the branch:

$$\Delta\omega_i = (|\omega_{i+1} - \omega_i| + |\omega_i - \omega_{i-1}|)/2. \quad (12)$$

In calculations we have used the CDS-1000 database on CO₂ molecule (see Ref. 13). The parameter $\Delta\omega_i$ is entered into reformatted database. The calculation of the central part of the contour for the case of CO₂ mixture with N₂ has some specific features as compared with that in the case of CO₂ mixture with He (see Refs. 11 and 12). Thus in Refs. 11 and 12 three parameters more are used from the reformatted database. As our calculations have shown the use of these parameters in the case of CO₂ mixture with N₂ is not that essential at high pressures. However, for commonness we have included one additional parameter too.

$$\theta_i = (|\omega_{i+1} - \omega_i| - |\omega_i - \omega_{i-1}|)/\Delta\omega_i. \quad (13)$$

It presents the relative change of the distance between the neighbor lines within the branch. We have introduced it as its application enables one to improve description of the absorption spectrum within the branch at relatively low pressures, like those considered, for example, in Ref. 6. It affects the asymptotic half-width, which transforms as follows

$$\xi_i^a(p) = \xi_i^a(p) \exp(B\theta_i) \quad (14)$$

with the parameter B being a positive value. Figure 2 presents the final value of the asymptotic half-width ξ_{fin}^a (7) calculated from the initial value ξ_{init}^a by formula (14) with the parameter $B = 1.5$. Another specific feature is that calculations for the mixture of the carbon dioxide with nitrogen require different, than in the case of mixture with helium, parameterizations of the factor-function (5) for different pressures.

To evaluate the half-widths from their values at 1000 K temperatures to T near normal values of 296 K, we made use of the simple power law with the exponent of 0.5:

$$\gamma_i^{0.5}(N_2, 1 \text{ atm}, T) = \gamma_i^L(N_2, 1 \text{ atm}, 1000 \text{ K})(1000/T)^{0.5}.$$

This formula is not a rigorous law and not always it is confirmed experimentally. Moreover, the dependence of the half-width we have proposed is essentially nonlinear. For these reasons the values of the Lorentzian half-width of an isolated line having non-Lorentzian contour is considered, in our calculations, as a parameter and not a constant. Its value is found from experimental data obtained at low pressures and to take it into account, we have introduced an additional scaling coefficient k :

$$\gamma_i^L(N_2, 1 \text{ atm}) = k_{N_2/N_2} \gamma_i^{0.5}(N_2, 1 \text{ atm}, 296 \text{ K}).$$

This coefficient has to bring the calculated behavior of the branch or band shape into agreement with those calculated earlier in papers, like Ref. 6, devoted to detailed analysis of the half-widths. In this calculations this coefficient was taken to be 1.4, in contrast to calculations of broadening by helium in Refs. 11 and 12, where its value was close to unity.

Modeling of the CO₂ absorption spectra performed for the cases with different broadening agents and temperatures while in the same schemes and same parameters of contours showed that some spectra have to depend on temperature in order to exhibit, when calculated, an adequate absorption at the peak of absorption branch. As a result, we have arrived at a conclusion that the parameter A in expression (11) is to be parameterized as follows:

$$A(T) = A(296 \text{ K})(296/T)^{1/2}.$$

Our calculations (see Fig. 3) made for relatively high pressures confirm the efficiency of the calculation scheme presented by expressions (1) and (2), in which the shape of an individual line (1) is modeled by use of parameters from Fig. 1 and Lorentzian contour L_i set by expressions (1) and (2) with its half-width being dependent on pressure in a specific way (see Fig. 2).

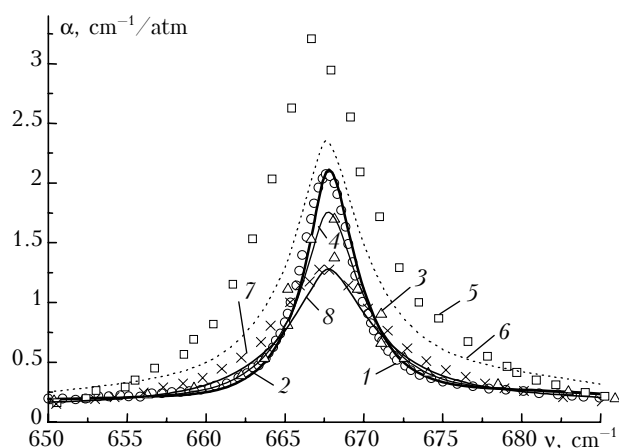


Fig. 3. Comparison of the calculated contour of the Q -branch of ν_2 absorption band of CO₂ with the data from Ref. 3: 1, 3, 5, 7 present experimental data³; 2, 4, 6, 8 show our calculated data; 1, 2 are for $T=296$ K and $p=70$ atm; 3, 4 for $T=296$ K and $p=100$ atm; 5, 6 for 198 K and 105 atm; 7, 8 for $T=296$ K and $p=200$ atm.

In Fig. 3 we compare our calculated data with the experimental data from Ref. 3 which was devoted to studying the absorption within wide interval in the ν_2 absorption band. Overall, the absorption within the Q -branch is reconstructed quite well for pressures from 70 to 200 atm, except for some discrepancies.

First, a certain shift of the central frequency of the contour toward higher values is observed, as compared with the experimental one. To a certain extent this shift is caused by the transformation (14)

applied. However, switching it off only insignificantly improves the situation, and does not completely restore the central frequency of the branch. On the contrary, in studying the mixture of CO₂ and helium in our previous papers^{11,12} we had to introduce, additionally, two parameters from the relevant database, while in the case of CO₂ mixture with N₂ at high pressures no additional parameters are needed at all, except for the spectral distance between the lines (see expression (12)).

Second, some excess absorption occurs in calculations at the edges of the Q -branch, which can be corrected by a proper modeling using refined parameters of the pointwise set function (5). However, no such calculations are presented here as this noticeably distorts the shape of individual line (see Fig. 1) in its wing that matters in the exponential presentation of the wing.

In our opinion the most serious shortcoming is in poor quality of modeling of the branch contour at a low temperature, 198 K (see Fig. 3). We didn't manage to remove this drawback completely even when strongly modifying the line shape. Perhaps, more detailed understanding is needed of the line shape formation in the transition region between its central part and the wing.

Now some words are to be said on the values of parameters used in modeling. The value A in expression (11) equals 4.5 and 46.0 for the asymptotic straight lines $\xi^{a,I}$ and $\xi^{a,II}$ in Fig. 2. This value is used in determination, by formula (11), of the ξ_0^a value from expression (7). To do this, one has to know the mean spectral distance (12) between the neighbor lines within the branch. Thus, for the Q_{30} line it equals 0.1257 cm^{-1} . The slope of the two straight lines in Fig. 2 is determined by the r parameter from expression (7), which correspondingly equals 0.52 and 0.10.

3. Calculations in the far wings of the line shapes

To calculate the absorption by carbon dioxide within the transmission windows of its absorption spectrum, the contour of an absorption line (1) was normally used in combination with the exponential temperature dependent factors (3) and (4). On the whole there is observed a good agreement between the reduced absorption coefficient values we have calculated ourselves with the experimental ones from Ref. 3 measured within a wide spectral region from 550 to 1100 cm^{-1} (see Fig. 4).

It is seen that the absorption calculated without the account of absorption in the far wings (see Fig. 5) is too overestimated.

The temperature behavior of the contour is quite adequate practically everywhere in the spectral interval considered, except for that in the far wings. In the central part of the contour ($640\text{--}680 \text{ cm}^{-1}$) the absorption calculated decreases with the increasing

temperature, while in the near wing (680–760 cm^{-1}) it, on the contrary, is higher for higher temperatures (see Fig. 5). In the far wings, (760–820 cm^{-1}), one can see³ that the absorption calculated for different temperatures has close values (see Fig. 5), though the behavior of the middle portion of the wing keeps, in our calculations, up to 1100 cm^{-1} . It is interesting to note that the parameter N in expressions (3) and (4) equals to 5, as in all our earlier calculations^{10,12} made for different spectral intervals.

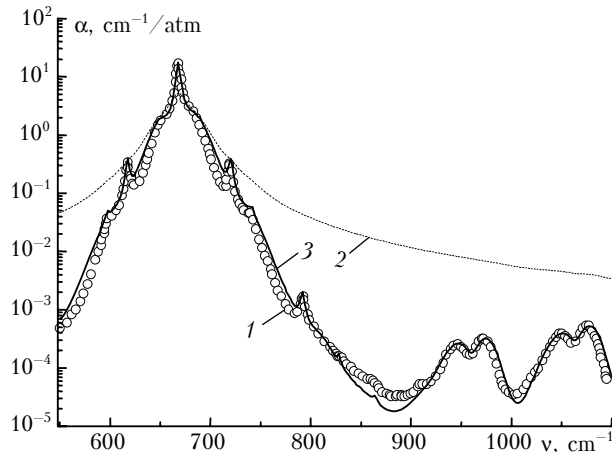


Fig. 4. Comparison of the reduced absorption coefficients of carbon dioxide calculated for the spectral region of the ν_2 absorption band³ at $p = 100$ atm and $T = 296$ K: experiment from Ref. 3 (1); data calculated using a Lorentzian (2); our calculations (3).

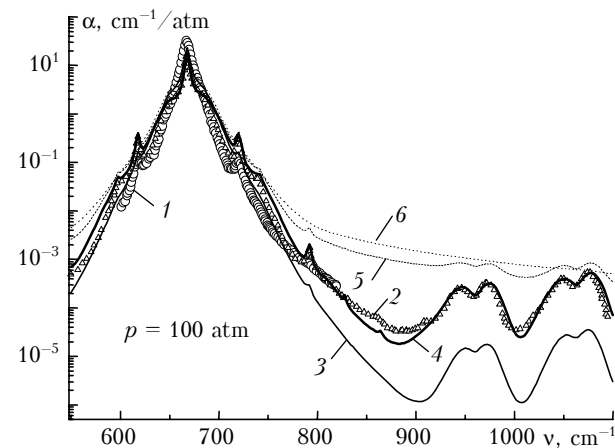


Fig. 5. The same as in Fig. 4; experimental data from Ref. 3 ($T = 198$ K, $p = 105$ atm (1); 296 K, 100 atm (2)); (198 K, 105 atm (3); 296 K, 100 atm (4)); data calculated with no account of the exponential factor (296 K, 100 atm (5); 198 K, 105 atm (6)).

Modeling the absorption at different pressures also has some interesting features. As seen from the experimental data³ presented in Fig. 6, the reduced absorption calculated for far wings of the Q -branch only weakly depends on pressure, though in our calculations it is proportional to the pressure of a buffer gas.

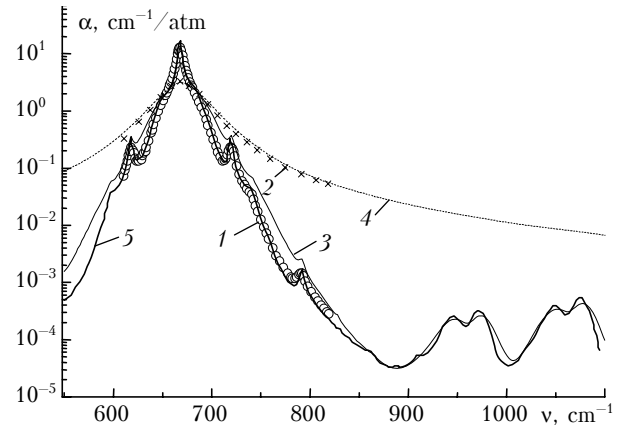


Fig. 6. The same as in Fig. 4, but for $T = 296$ K and $p = 200$ atm; experimental data from Ref. 3 ($p = 200$ atm (1); 100 atm (5)); data³ calculated using the Lorentzian (2); our calculations (3); our calculations with the use of Lorentzian (4).

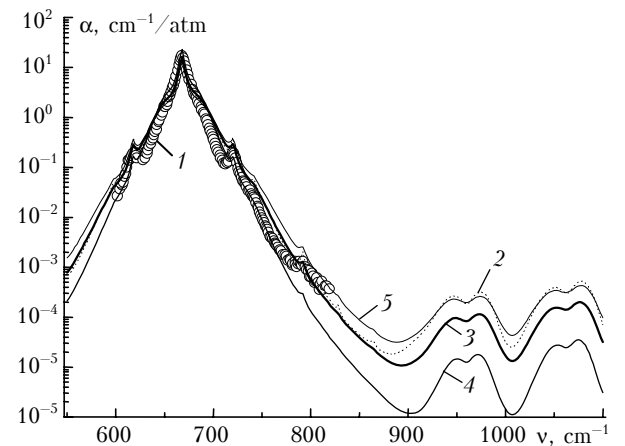


Fig. 7. The same as in Fig. 4, but for $T = 255$ K and $p = 159$ atm. For a convenience we present here our data calculated for other conditions: experimental data³ for $T = 255$ K, $p = 159$ atm (1); our calculations 296 K, 100 atm (2); 255 K, 159 atm (3); 198 K, 105 atm (4); 296 K, 200 atm (5).

Our calculation technique has been polished in calculations for different spectral regions, where the absorption in the far wings is proportional to the squared pressure of the gas itself or a buffer gas. For a certain combination of the ambient conditions, for example at $T = 255$ K and $p = 159$ atm, the calculated absorption (Fig. 7) only slightly differs from that at $T = 296$ K and $p = 100$ atm (see Fig. 4) in the spectral range up to 880 cm^{-1} . This well agrees with the experimental data, especially if taking into account the fact that the pressure and temperature behaviors of the absorption are of the inverse character.

4. General discussion and concluding remarks

On the whole, I can state that this paper brings out the usefulness of the line-by-line calculation technique for the case of an absorption band at high

pressures by use of non-Lorentzian pressure behavior of the contour of an individual line. It is well known that no isolated line exists and that this circumstance is the main cause why the problem on the line shape cannot be solved experimentally. To achieve this task, one has to make certain assumptions and it is quite desirable that modeling is used for understanding the main properties of the absorption. In this paper only one simple scheme of calculations has been considered from other possible approaches to such a modeling. This scheme shows that, to realize the line-by-line calculation technique, one can build up a contour of an isolated line (see Fig. 1) from the Lorentzian one such that its half-width becomes a linear function of the pressure (see Fig. 2).

Obviously, the characteristic pressure dependence of the line half-width is quite understandable. Really, a molecule cannot instantly change its energy state after absorbing or emitting a photon. Some time is needed for the energy to be redistributed over the internal degrees of freedom, with this redistribution being governed by such molecular characteristics as molecular momentum, for instance. The additional collisions that happen during the transition do not fully modify its relaxation properties or the line half-width, as it happens at low pressures. The explanation of an individual line collapse (see Fig. 1) seems to be not that simple. One can suppose that its formation not necessarily follows from the temporal correlations occurring if using the equations of motion of the colliding molecules and may allow one to consider the photon interactions in the spectra of stimulated emission and absorption.

The simplicity of the scheme proposed is quite advantageous in calculating absorption spectra in wide spectral regions, which is important for atmospheric applications in climate studies as well as in constructing the overview spectra. Nevertheless, this scheme can successfully be applied to calculations in problems on sensing within narrow spectral intervals, though this would require refining the parameters we used in this paper in order to adapt the shape of an individual line in application to the particular band or branch chosen.

Of course, further investigations into the absorption in the far line wings are needed. Although no experimental data are available on the absorption in the far wing of the Q-branch behind 820 cm^{-1} at other temperatures (see Fig. 4) and the measurement accuracy in this region is lower, according to opinion of the authors of the experimental study in Ref. 3, there is a tendency seen in our studies toward poorer

agreement of our results with the experiments at the temperature of 198 K. It is quite possible that this interval, as well as the regions of other absorption bands, is covered by the continuum absorption, which, as a rule is characterized by the inverse temperature behavior of the absorption. It is extremely important to obtain new experimental data on the absorption in the regions of other absorption bands of the carbon dioxide for studying the dependence of absorption on temperature and pressure of a buffer gas.

References

1. D.D. Turner, D.C. Tobin, S.A. Clough, P.D. Brown, R.G. Ellingson, E.J. Mlawer, R.O. Knuteson, H.E. Revercomb, T.R. Shippert, and W.L. Smith, *J. Atmos. Sci.* **61**, 2657–2675 (2004).
2. S.A. Tjemkes, T. Patterson, R. Rizzi, M.W. Shephard, S.A. Clough, M. Matricardi, J.D. Haigh, M. Hopfner, S. Payan, A. Trotsenko, N. Scott, P. Rayer, J.P. Taylor, C. Clerbaux, L.L. Strow, S. DeSouza-Machado, D. Tobin, and R. Knuteson, *J. Quant. Spectrosc. Radiat. Transfer* **77**, No. 4, 433–453 (2003).
3. F. Niro, C. Boulet, and J.-M. Hartmann, *J. Quant. Spectrosc. Radiat. Transfer* **88**, 483–498 (2004).
4. F. Niro, F. Hase, C. Camy-Peyret, S. Payan, and J.-M. Hartmann, *J. Quant. Spectrosc. Radiat. Transfer* **90**, No. 1, 43–59 (2005).
5. F. Niro, von T. Clarmann, K. Jucks, and J.-M. Hartmann, *J. Quant. Spectrosc. Radiat. Transfer* **90**, No. 1, 61–76 (2005).
6. R. Rodrigues, K.W. Jucks, N. Lacombe, Gh. Blanquet, J. Walrand, W.A. Traub, B. Khalil, R. Le Doucen, A. Valentin, C. Camy-Peyret, L. Bonamy, and J.-M. Hartmann, *J. Quant. Spectrosc. Radiat. Transfer* **61**, No. 2, 153–184 (1999).
7. K.W. Jucks, R. Rodrigues, R. Le Doucen, C. Claveau, W.A. Traub, and J.-M. Hartmann, *J. Quant. Spectrosc. Radiat. Transfer* **63**, No. 1, 31–48 (1999).
8. L. Ozanne, Nguyen-Van-Thanh, C. Brodbeck, J.P. Bouanich, J.-M. Hartmann, and C. Boulet, *J. Chem. Phys.* **102**, No. 19, 7306–7316 (1995).
9. J. Boissoles, F. Thibault, and C. Boulet *J. Quant. Spectrosc. Radiat. Transfer* **56**, No. 6, 835–853 (1996).
10. V.F. Golovko, *Atmos. Oceanic Opt.* **14**, No. 9, 807–812 (2001).
11. V.F. Golovko, *Proc. SPIE* **5396**, 11–22 (2003).
12. V.F. Golovko, in: *Optical Spectroscopy and Frequency Standards. Molecular Spectroscopy*, Ed. by L.N. Sinitisa and E.A. Vinogradov (Publishing House of IAO SB RAS, Tomsk, 2004), P. 437–465 and 473–476.
13. S.A. Tashkun, V.I. Perevalov, J.-L. Teffo, A.D. Bykov, and N.N. Lavrentieva, *J. Quant. Spectrosc. Radiat. Transfer* **82**, Nos. 1–4, 165–197 (2003).